Available online at www.sciencedirect.com
ScienceDirect
Inorganica Chimica Acta 360 (2007) 546–556
Inorganica Chimica Acta
www.elsevier.com/locate/ica

Interaction of Fe(III) with herbicide-carboxylato ligands. Di-, tri- and tetra-nuclear compounds: Structure, antimicrobial study and DNA interaction

Anastasia Dimitrakopoulou [a], Catherine Dendrinou-Samara [a], Anastasia A. Pantazaki [d], Catherine Raptopoulou [b], Aris Terzis [b], Elias Samaras [c], Dimitris P. Kessissoglou [a,*]

[a] *Department of General and Inorganic Chemistry, Aristotle University of Thessaloniki, Thessaloniki 54124, Greece*
[b] *NCSR "Demokritos", Institute of Materials Science, 15310 Aghia Paraskevi Attikis, Greece*
[c] *Laboratory of Biotechnology, Technological Educational Institution, Sindos, Thessaloniki, Greece*
[d] *Laboratory of Biochemistry, Department of Chemistry, Aristotle University of Thessaloniki, Thessaloniki 54124, Greece*

Received 4 July 2006; accepted 28 July 2006
Available online 12 August 2006

Abstract

The iron complexes with the phenoxyalkanoic acids 2,3-D = 2,3-dichlorophenoxyacetic acid, 3,4-D = 3,4-dichlorophenoxyacetic acid, 2,4,5-T = 2,4,5-trichlorophenoxyacetic acid, and mcpa = 2-chloro-4-methyl-phenoxyacetic acid, in the presence or not of a nitrogen donor heterocyclic ligand, py = pyridine, bipy = 2,2′ bipyridine, phen = 1,10-phenanthroline, were prepared and characterized.The interaction of Fe(III) with phenoxyalkanoic acids and bipy or phen leads to dinuclear neutral complexes, while the presence of py favors tetranuclear neutral forms. The crystal structures of $[Fe_2OCl_2(mcpa)_2(bipy)_2]\cdot 0.25(bipy)\cdot 0.8MeCN$ (**1a**), and $\{[Fe_4O_2(mcpa)_6Cl_2(py)_4]\cdot 2MeCN\}$ (**3a**), have been determined. DNA–Fe(III) complex interaction studies suggest that iron complexes promote the hydrolytic cleavage of double stranded DNA that seems to be oxygen independent, while pDNA shows cross-linking with many molecules of the iron clusters. Antibacterial screening data showed that the presence of chelating agents, bipy or phen, increased the efficiency of iron complexes.
© 2006 Elsevier B.V. All rights reserved.

Keywords: Iron(III) complexes; Phenoxyalkanoic acids; DNA interaction; Antimicrobial behaviour

1. Introduction

In the bioinorganic area, iron hydroxo- and oxo-bridged dinuclear complexes represent synthetic models of the active sites of various non-heme iron proteins such as hemerythrin (Hr), ribonucleotide reductase R2 protein (RNR-R2), methane monooxygenase (MMOH) or purple acid phosphatases (PAPs) which contain diiron cores bridged by oxo or hydroxo ligands, while polynuclear Fe(III)/O^{2-}, OH^- complexes represent model systems for the iron-oxo core of ferritin and for the biomineralization processes that form a variety of iron/oxo minerals [1–9]. The ability of the ligand systems RCO_2^-/L (L = neutral bidentate N-donor) to assemble novel Fe(III) cluster exhibiting interesting structures and magnetic phenomena has been investigated [10–12].

Dinuclear Fe(III) complexes are known in neutral and cationic forms [13–23]. This class of compounds can be characterized by the presence of [Fe_2–(μ-O)] core, while carboxylato groups can also bridge the two metal ions e.g. $[Fe_2O(O_2CMe)_2Cl_2(bpy)_2]$ [13], $[Fe_2O(O_2CCH_2Cl)_2(H_2O)(bpy)_2](NO_3)_2$ [15], $[Fe_2O(O_2CCF_3)_2(Me_2bpy)_4](ClO_4)_2$ [16], $[Fe_2O(O_2CPh)_2(phen)_4]Cl_2$ [17].

Oxo-centered, carboxylato-bridged trinuclear iron complexes [24–27] having the [Fe_3–(μ-O)] core have been characterized in mixed valence $Fe(III)_2Fe(II)$ [26] or

* Corresponding author. Tel.: +30 23 10997723; fax: +30 23 10997738.
E-mail address: kessisog@chem.auth.gr (D.P. Kessissoglou).

0020-1693/$ - see front matter © 2006 Elsevier B.V. All rights reserved.
doi:10.1016/j.ica.2006.07.102

homovalence $Fe(III)_3$ mono-cationic clusters with the general formula $[Fe_3O(O_2CR)_6(solvent)_3](X)_{0\text{ or }1}$ [25]. The tetranuclear oxo-bridged carboxylato compounds include three types of butterfly motifs [28–32], the "bent" with the pyramidal μ_3-O ions on the same side or on the opposite sides of the fused Fe_3 planes [31–36] or "planar" [37–39], while examples having the rectangular core have also been reported [40].

Dinuclear iron complexes are capable of promoting the hydrolytic cleavage of plasmid DNA under aerobic and anaerobic conditions, producing single and double DNA strand breaks at biological pH values [41–43]. Spectroscopic titrations of iron clusters with calf thymus DNA have also been used to evaluate the binding to the DNA helix [44–46].The studies reported by Norden and co-workers investigated the "Pfeiffer effect" induced by the interaction of Fe(II) compounds of bipy and phen with double helical DNA [47–49] while, the DNA binding studies of mixed-ligand complexes having Fe(II) as a central atom have attracted limited attention [50–56].

Our interest is focused on the interaction of metal ion with carboxylato ligands. We have initiated studies on the coordination chemistry of herbicide-carboxylato agents with Cu(II), Mn(II), Mn(III), Ni(II) and d^{10} ions in an attempt to examine their mode of binding and possible biological relevance [57–61]. We have also reported [62,63] studies on the effect of polynuclear Ni(II) complexes on the integrity and electrophoretic mobility of nucleic acids. The antifungal and antibacterial properties of a range of metal complexes have been evaluated against several pathogenic fungi and bacteria [64–75].

In this paper, we report the synthesis and characterization of binuclear, trinuclear and tetranuclear Fe(III) carboxylato compounds with the commercial auxin herbicides, 2,3-D, 3,4-D, 2,4,5-T and mcpa (Scheme 1) in the presence or not of phen, bipy or py. We also report the molecular and the crystal structures of bis(bipyridine)dichlorobis(2-chloro-4-methyl-phenoxyacetato)oxodi-iron(III), $[Fe_2OCl_2(mcpa)_2(bipy)_2]\cdot 0.25(bipy)\cdot 0.8MeCN$ (**1a**) and dichlorotetrakis(pyridine) hexakis(2-chloro-4-methyl-phenoxyacetato)dioxotetrairon(III) acetonitrile(1/2), $\{[Fe_4O_2(mcpa)_6Cl_2(py)_4]\cdot 2MeCN\}$ (**3a**). All nuclearities of iron complexes were tested for their interaction or hydrolysis abilities towards native dsDNA and pDNA. Furthermore, DNA binding studies by spectroscopic titration have been performed. Minimum inhibitory concentrations (MIC) against four different bacteria species of the Fe(III) complexes with the commercially available auxin herbicides 2,4,5-T, 3,4-D, mcpa and 2,3-D were also measured.

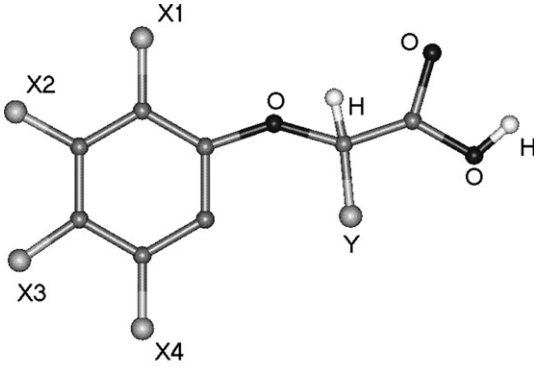

2,4,5-T: X_1 = Cl, X_2 = H, X_3 = Cl, X_4 = Cl, Y = H

3,4-D: X_1 = H, X_2 = Cl, X_3 = Cl, X_4 = H, Y = H

2,3-D: X_1 = Cl, X_2 = Cl, X_3 = H, X_4 = H, Y = H

mcpa: X_1 = CH_3, X_2 = H, X_3 = Cl, X_4 = H, Y = H

Scheme 1. Formulas of the alkanoic acids used.

2. Experimental

2.1. Materials

The chemicals for the synthesis of the compounds were used as purchased. Acetonitrile (CH_3CN) was distilled over calcium hydride (CaH_2) and CH_3OH over magnesium (Mg) and was stored over 3 Å molecular sieves. Diethyl ether, anhydrous grade, dimethylformamide = dmf and dimethylsulfoxide = dmso were used without any further purification. 3,4-D, 2,3-D, 2,4,5-T, mcpa, phen, bipy, py and $FeCl_3\cdot 6H_2O$ were purchased from Aldrich Co. All chemicals and solvents were of reagent grade. Agarose was purchased from BRL. Tryptone and yeast extract were purchased from Oxoid (Unipath LTD, Hampshire, UK). Native DNA (dsDNA) (CTDNA) from calf thymus gland was purchased from Sigma.

2.2. Preparation of the complexes

All the compounds reported here have been prepared according to the general procedure described below, while spectroscopic data and elemental analysis of all the compounds tested for the biological relevance are given as Supplementary data.

2.2.1. Synthesis of the binuclear Fe(III) complexes

General procedure: 10 mmol of a phenoxyalkanoic acid were dissolved in CH_3OH or CH_3CN (20 cm^3) and 10 mmol of NaOH (0.40 g) was added. After 30 min of stirring, 10 mmol of $FeCl_3\cdot 6H_2O$ (2.7 g) in CH_3OH or CH_3CN (15 cm^3) and 10 mmol of phen in CH_3OH or bipy in CH_3CN (10 cm^3) were added dropwise. The reaction mixture was stirred for an additional 30 min. The brown-green solution was reduced in volume and left for slow evaporation. Small green crystals or green microcrystalline solids of the compounds, $[Fe_2OCl_2(mcpa)_2(bipy)_2]\cdot 0.25(bipy)\cdot 0.8MeCN$ (**1a**), $[Fe_2OCl_2(2,4,5\text{-}T)_2(bipy)_2]$ (**1b**), $[Fe_2OCl_2(3,4\text{-}D)_2(bipy)_2]$ (**1c**), $\{[Fe_2OCl_2(2,4,5\text{-}T)_2(phen)_2]\cdot H_2O\cdot 3MeOH\}$ (**1d**), $\{[Fe_2OCl_2(mcpa)_2(phen)_2]\cdot H_2O\cdot 3MeOH\}$ (**1e**), $\{[Fe_2OCl_2(3,4\text{-}D)_2(phen)_2]\cdot H_2O\cdot 3.5MeOH\}$ (**1f**) [76], were deposited in 2–5 days.

*2.2.1.1. Synthesis of the bis(bipyridine)dichlorobis(2-chloro-4-methyl-phenoxyacetato)oxodi-iron(III) [$Fe_2OCl_2(mcpa)_2(bipy)_2$] · 0.25(bipy) · 0.8MeCN (**1a**).* Green crystals of **1a** suitable for X-ray structure determination were deposited from acetonitrile solution in 4 days. Yield 65%. (Fw = 982.09). (Found: C, 51.25; H, 3.75; N, 7.25; Fe 11.20; $C_{42.1}H_{36.4}Cl_4Fe_2N_{5.3}O_7$ requires C, 51.44; H, 3.71; N, 7.55; Fe, 11.40); IR: ν_{max}/cm^{-1} ν_{bipy}(C=N): 1606 (vs); $\nu_{as}(CO_2)$: 1597 (vs); $\nu_{sym}(CO_2)$: 1419 (s) (KBr pellet); UV–Vis: λ (nm) (ε, $dm^3\,mol^{-1}\,cm^{-1}$), dmso solution: 530 (720); 480 (1200); 361 (3100).

2.2.2. Synthesis of the trinuclear Fe(III) complexes

General procedure: 10 mmol of a phenoxyalkanoic acid in CH_3OH (15 cm^3) and 10 mmol of NaOH (0.4 g) were added. After 30 min of stirring, 5 mmol of $FeCl_3 \cdot 6H_2O$ (1.35 g) in CH_3OH (10 cm^3) was added dropwise. The orange-yellow solution was reduced in volume and left for slow evaporation. The orange-yellow crystalline solid of the compounds, $[Fe_3O(2,3\text{-}D)_6(MeOH)_3]Cl \cdot 3MeOH$ (**2a**) [76], $[Fe_3O(3,4\text{-}D)_6(MeOH)_3]Cl \cdot 3MeOH$ (**2b**), $[Fe_3O(2,4,5\text{-}T)_6(MeOH)_3]Cl \cdot 3MeOH$ (**2c**) were deposited in 2–3 days.

2.2.3. Synthesis of the tetranuclear Fe(III) complexes

General procedure: 10 mmol of a phenoxyalkanoic acid was dissolved in CH_3OH/dmso 1:1 or CH_3CN (20 cm^3) and 10 mmol of NaOH (0.4 g) was added. After 30 min stirring, 5 mmol of $FeCl_3 \cdot 6H_2O$ (1.35 g) in CH_3OH/dmso 1:1 or CH_3CN/pyridine 3:1 (10 cm^3) was added dropwise. The reaction mixture was stirred for an additional 1 h and reduced in volume under vacuum and left for slow evaporation. Red-cognac crystalline solid of the compounds, $\{[Fe_4O_2(mcpa)_6Cl_2(py)_4] \cdot 2MeCN\}$ (**3a**), $\{[Fe_4O_2(2,4,5\text{-}T)_6Cl_2(py)_4] \cdot 2MeCN\}$ (**3b**), $\{[Fe_4O_2(3,4\text{-}D)_6Cl_2(py)_4] \cdot 2MeCN\}$ (**3c**), $\{[Fe_4O_2(2,4,5\text{-}T)_8(dmso)_4] \cdot 2MeOH \cdot H_2O \cdot 0.8dmso\}$ (**3d**) [76], $\{[Fe_4O_2(2,3\text{-}D)_8(dmso)_4] \cdot 2MeOH \cdot H_2O \cdot dmso\}$ (**3e**), $\{[Fe_4O_2(3,4\text{-}D)_8(dmso)_4] \cdot 2MeOH \cdot H_2O \cdot dmso\}$ (**3f**) were deposited in 2–5 days.

*2.2.3.1. Synthesis of the dichlorotetrakis(pyridine)-hexakis(2-chloro-4-methyl-phenoxyacetato) dioxotetrairon-(III)acetonitrile(1/2), {[$Fe_4O_2(mcpa)_6Cl_2(py)_4$]2MeCN} (**3a**).* Red-cognac crystals of **3a**, suitable for X-ray structure determination, were deposited from CH_3CN/pyridine 3:1 solution in 2 days. Yield 60%. (Fw = 1922.43). (Found: C, 48.54; H, 3.78; N, 4.16; Fe, 11.46; $C_{78}H_{74}Cl_8Fe_4N_6O_2$ requires, C, 48.68; H, 3.84; N, 4.36; Fe, 11.61) IR: ν_{max}/cm^{-1} ν_{py}(C=N): 1606 (vs); $\nu_{as}(CO_2)$: 1600 (vs); $\nu_{sym}(CO_2)$: 1420 (vs) (KBr pellet); UV–Vis: λ (nm) (ε, $dm^3\,mol^{-1}\,cm^{-1}$), dmso solution: 582 (197); 468 (660).

2.3. Methods

Infrared spectra (200–4000 cm^{-1}) were recorded on a Perkin–Elmer FT-IR 1650 spectrometer with samples prepared as KBr pellets. UV–Vis spectra were recorded on a Shimadzu-160A dual beam spectrophotometer. C, H and N elemental analyse were performed on a Perkin–Elmer 240B elemental analyzer, Fe was determined by atomic absorption spectroscopy on a Perkin–Elmer 1100B spectrophotometer. Electric conductance measurements were carried out with a WTW model LF 530 conductivity outfit and a type C cell, which had a cell constant of 0.996. This represents a mean value calibrated at 25 °C with potassium chloride. All temperatures were controlled with an accuracy of ±0.1 °C using a Haake thermoelectric circulating system.

2.4. Antimicrobial activity

The antimicrobial efficiency of the complexes was tested by their ability to inhibit the growth of microorganisms in the cultivation medium Mueller–Hinton broth (Imuna). The tests were performed according to minimum inhibitory concentration (MIC) in μg/mL with four bacteria species: *Staphylococcus aureus*, *Escherichia coli*, *Bacillus subtilis* and *Proteus bulgaris*. The concentration of microorganisms in the cultivation medium was 10^5–10^6 cfu/mL.The concentrations of 1600, 800, 400, 200, 100, 50, 25, 12.5, 6.25 μg/mL of the complexes in propyleneglycol were tested and the minimum inhibitory concentrations (MIC) were determined.

2.5. Plasmid isolation

Plasmid pUC119 was isolated from *E. coli XL1* by the alkaline SDS lysis method (Strategene). All plastics and glassware used in the experiments with nucleic acids were autoclaved for 30 min at 120 °C and 130 kPa. The heat-resistant solutions were similarly treated, while heat-sensitive reagents were sterilized by a filter.

2.6. Agarose gel electrophoresis of nucleic acids

Aliquots of 3–5 μg of each nucleic acid were incubated in the presence of iron compounds in a final volume of 20 μL. The reaction mixture was incubated for 30 min at a constant temperature of 37 °C and the reaction was terminated by the addition of 5 μL loading buffer consisting of 0.25% bromophenol blue, 0.25% xylene cyanol FF and 30% glycerol in water. The products resulting by the DNA–compound interactions were separated by electrophoresis on agarose gels (1% w/v), containing 1 μg/mL ethidium bromide in 40 mM Tris–acetate, pH 7.5, 20 mM sodium acetate, 2 mM Na_2EDTA, at 5 V/cm. Agarose gel electrophoresis was performed in a horizontal gel apparatus (Mini-Sub™ DNA Cell, Bio-Rad) for about 4 h. Since ethidium bromide forms a fluorescent complex when it binds to DNA, a decreased of fluorescence signifies diminution of the amount of DNA. The gels were visualized in the presence of UV light.

2.7. Artificial nucleolytic enzyme activity assay

The assay for measuring the potential hydrolytic cleavage of phosphodiester–DNA bonds (artificial deoxyribonucleolytic activity) was based on the conversion of free nucleic acid to an acid soluble form after the addition of perchloric acid and centrifugation. Therefore, in the supernatant remained the oligonucleotides derived from the DNA degradation or the free iron complex, while in the pellet remained the high molecular weight molecules, including the non-degraded DNA substrate (or polynucleotides) and the potential DNA–iron complex.

Thus, artificial deoxyribonucleolytic activity was assayed at 37 °C in a total volume of 0.5 mL in the presence of the iron complex, DNA (0.6 mg/mL) and 50 mM of Tris–Cl buffer (pH 7.5 measured at 25 °C). The reactions were terminated, by adding an equal volume of chilled 12.5% (v/v) perchloric acid. The experimental apparatus was held in an ice bath for 10 min to precipitate the high molecular weight molecules removed by centrifugation at 4 °C (15 min; 12,500*g*). The absorbance of the acid soluble products was measured at 260 nm.

2.8. X-ray crystal structure determination

A green parallelepiped crystal of $[Fe_2OCl_2(mcpa)_2(bipy)_2]\cdot 0.25(bipy)\cdot 0.8MeCN$ (**1a**) with approximate dimensions $0.10\times0.20\times0.50$ mm and a red one of $\{[Fe_4O_2(mcpa)_6Cl_2(py)_4]\cdot 2MeCN\}$ (**3a**), with approximate dimensions $0.12\times0.13\times0.70$ mm were mounted in air. Diffraction measurements were made on a Crystal Logic Dual Goniometer diffractometer using graphite monochromated Mo radiation.The crystal data and parameters for data collection are reported in Table 1.The unit cell dimensions were determined and refined by using the angular settings of 25 automatically centered reflections. Intensity data were recorded using θ–2θ scan. Three standard reflections monitored every 97 reflections, showed <3.0% intensity fluctuation and no decay. Lorentz, polarization and ψ-scan absorption correction were applied using Crystal Logic software. Scattering factors were taken from the International Tables for X-ray Crystallography [79].

Table 1
Summary of crystal, intensity collection and refinement data

	1a	**3a**
Formula	$C_{42.1}H_{36.4}Cl_4Fe_2N_{5.3}O_7$	$C_{78}H_{74}Cl_8Fe_4N_6O_{20}$
Fw	982.07	1922.43
T (K)	298	293(2)
Crystal system	monoclinic	triclinic
Space group	$C2/c$	$P\bar{1}$
a (Å)	25.14(1)	15.113(6)
b (Å)	23.25(1)	18.732(6)
c (Å)	16.543(8)	19.095(7)
α (°)	90	119.090(10)
β (°)	95.54(2)	100.770(10)
γ (°)	90	101.360(10)
Volume (Å^3)	9624(7)	4372(3)
Z	8	2
D_{calc} (Mg/m^3)	1.356	1.460
Absorption coefficient, μ (mm^{-1})	0.875	0.965
F(000)	4017	1968
θ Range	2.14–23.00	2.17–22.25
Goodness-of-fit on F^2	1.052	1.026
R_1	0.0551[a]	0.0428[b]
wR_2	0.1571[a]	0.1046[b]

[a] 5300 reflections with $I>2\sigma(I)$.
[b] For 7969 reflections with $I>2\sigma(I)$.

The structures of **1a** and **3a** were solved by Direct methods using the programs SHELXS86 [80], and refined by the full-matrix least-squares techniques on F^2 with SHELXL-97 [81].

Further crystallographic details can be found at CIF files for **1a** (CCDC 297100) and **3a** (CCDC 297101) and were deposited as Supplementary data.

3. Results and discussion

3.1. Synthesis of the complexes

(a) The synthesis of the binuclear complexes has been achieved via the reaction of $FeCl_3\cdot 6H_2O$ with the sodium salts of the ligands in the presence of phen or bipy. e.g.,

$$2C_6H_3Cl_2\text{–}OCH_2COONa + 2FeCl_3 + 2NaOH + 2phen \rightarrow [Fe_2OCl_2(C_6H_3Cl_2\text{–}OCH_2COO)_2(phen)_2] + 4NaCl + H_2O$$

The complexes are green crystalline solids soluble in dmf, dmso.

(b) The synthesis of the trinuclear complexes has been achieved via the one step reaction of $FeCl_3\cdot 6H_2O$, NaOH, and 2,3-D that results in the formation of the cationic complex,

$$6C_6H_3Cl_2\text{–}OCH_2COOH + 8NaOH + 3FeCl_3 \rightarrow [Fe_3O(C_6H_3Cl_2\text{–}OCH_2COO)_6(MeOH)_3]Cl + 8NaCl + 7H_2O$$

The complexes are orange-yellow crystalline solids soluble in dmf, dmso.

(c) The synthesis of the tetranuclear complexes has been achieved via the reaction of $FeCl_3\cdot 6H_2O$ with the sodium salt of the ligand in dmso or CH_3CN + py e.g.,

$$8C_6H_2Cl_3\text{–}OCH_2COONa + 4FeCl_3 + 4NaOH \rightarrow [Fe_4O_2(C_6H_2Cl_3\text{–}OCH_2COO)_8(dmso)_4] + 12NaCl + 2H_2O$$

The complexes isolated from dmso are red-cognac crystalline solids while those from CH_3CN + py are red crystalline solids and all of them are soluble in dmf, dmso.

The formation of binuclear compounds is driven by the presence of chelating phen or bipy neutral ligands while

the formation of trinuclear or tetranuclear compounds is absolutely dependent on the solvent used. The use of methanol leads to the formation of the trinuclear species while from dmso, dmf or acetonitrile solvents in the presence or absence of py, the tetranuclear compounds have been isolated.

IR spectroscopy was used as an additional technique to distinguish the structural similarities of the compounds with the same nuclearity as well as the coordination mode of the carboxylato ligands. The overall patterns of all compounds of the same number of metal ions, bi-, tri- and tetra-Fe(III) ions are almost identical supporting analogous structures. The bands of phen or bipy in the 1650–1600 cm^{-1}, attributed to ring stretching vibrations, shift to higher frequencies upon chelation on binuclear compounds. Similar shifts occur for the bands between 1250 and 1100 cm^{-1}, while those between 1050 and 700 cm^{-1} shift to lower frequencies with splitting of the band at ~850 cm^{-1} (an out-of-plane C–H deformation). The very strong bands at the range 1600–1575 cm^{-1} are assigned to the ν_{as}(COO) bidendate mode while the strong bands about 1420 cm^{-1} are assigned to the ν_{s}(COO) bidentate mode, of the carboxylato ligands, respectively.

3.2. Description of the structure $[Fe_2OCl_2(mcpa)_2(bipy)_2]$ (**1a**)

A diagram of the complex $[Fe_2OCl_2(mcpa)_2(bipy)_2]$ (**1a**) appears in Fig. 1. The selected bond distances and angles are given in Table 2. Two μ_1, μ_2 bridging phenoxyalkanoato mcpa ligands in *syn–syn* mode and an μ-O^{2-} group form bridges between the Fe(III) atoms separated by 3.165 Å. The Fe(1)–O(21) = 1.786(3) Å and Fe(2)–O(21) = 1.791(3) Å distances are almost the same. The Fe(III) coordination geometry is of a slightly distorted octahedron with a chloro ligand and a carboxylato oxygen atom in the axial position, while the two bipy nitrogen atoms, an oxygen of a carboxylato ligand and the μ-O^{2-} atom form the meridional plane (average torsion angles = 178.2°). The iron atom of each octahedron lies slightly out of the meridional plane.

Table 2
Selected bond distances (Å) and angles (°) for complex **1a**

Bond distances (Å)			
Fe1–O21	1.786(3)	Fe2–O21	1.791(3)
Fe1–O1	2.034(3)	Fe2–O12	2.024(3)
Fe1–O11	2.121(3)	Fe2–O2	2.118(3)
Fe1–N1	2.146(4)	Fe2–N11	2.165(4)
Fe1–N2	2.224(4)	Fe2–N12	2.207(4)
Fe1–Cl1	2.359(2)	Fe2–Cl2	2.356(2)
Fe2–Fe1	3.165		
Angles (°)			
O1–Fe1–N1	157.7(2)	O21–Fe2–N12	167.0(2)
O21–Fe1–N2	171.2(2)	O12–Fe2–N11	163.9(1)
O11–Fe1–Cl1	170.09(9)	O2–Fe2–Cl2	163.28(9)
Fe2–O21–Fe1	124.5(2)		

In the lattice structure of **1a** there is also a bipy molecule sitting at the center of symmetry, which means that it is positionally disordered. It is also translationally disordered along the crystallographic *c* axis.

The Fe(III)–O–Fe(III) angle of 124.5(2)° and Fe(III)···Fe(III) separation of 3.165 Å fall in the range 120–124° and 3.090–3.160 Å, respectively, reported for analogous compounds [13]. The structure is similar to that reported by Vincent et al. [14], while the dinuclear core has been observed in a series of Fe(III) cationic units [13–17].

3.3. Description of the structure $\{[Fe_4O_2(mcpa)_6Cl_2(py)_4]\cdot 2MeCN\}$ (**3a**)

Complex **3a** crystallizes in the triclinic space group $P\bar{1}$.The structural diagram of the complex appears in Fig. 2. The selected bond distances and angles are given in Table 3.

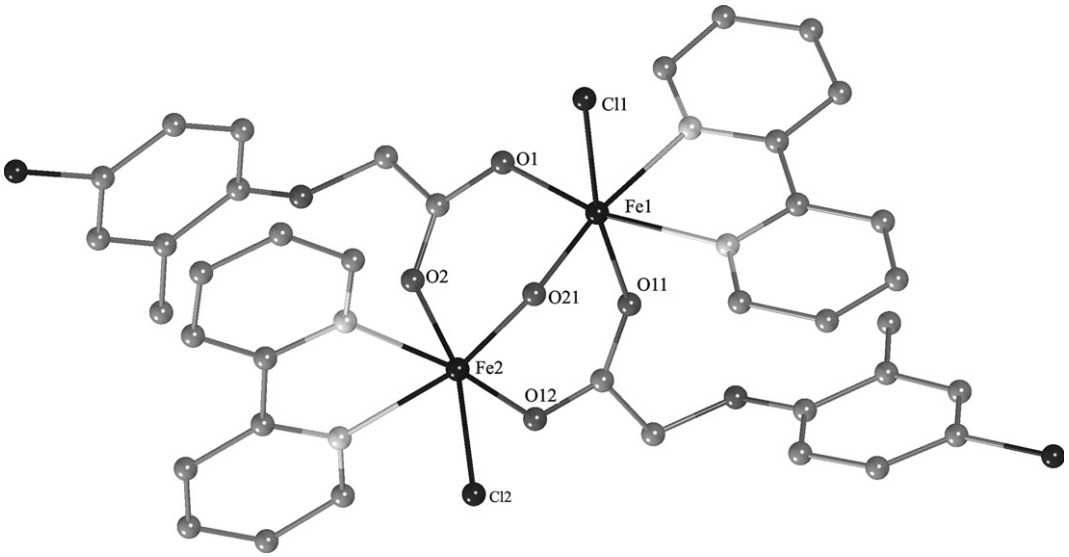

Fig. 1. A diagram of the structure of $[Fe_2OCl_2(mcpa)_2(bipy)_2]$ (**1a**).

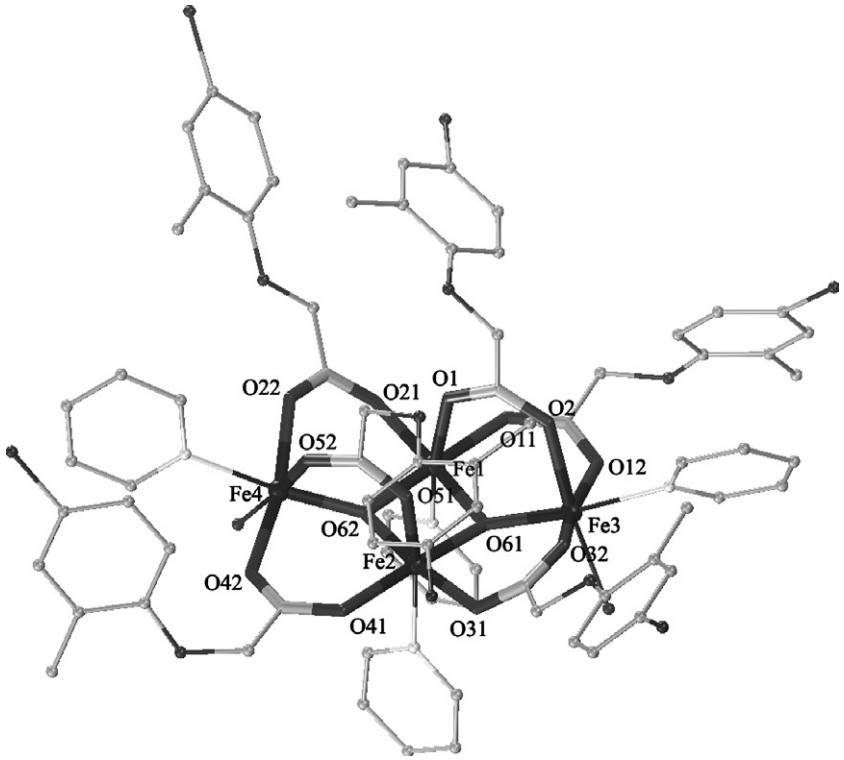

Fig. 2. A diagram of the structure of {[$Fe_4O_2(mcpa)_6Cl_2(py)_4$]· 2MeCN} (**3a**).

The tetranuclear molecule contains a $[Fe_4(\mu_3\text{-}O)_2]^{8+}$ core comprising four Fe(III) ions with a ''butterfly'' disposition and a μ_3-O^{2-} ion bridging each Fe_3 ''wing''. Ions Fe(1) and Fe(2) occupy the ''hinge'' or ''body'' sites, and Fe(3) and Fe(4) occupy the ''wing-tip'' sites. Both oxo ions, O(61) and O(62), lie slightly out of their respective Fe_3 planes by about 0.30 Å with a sum of angles of 352.87° and 352.69°, respectively. The torsion angle between the two Fe_3 planes is 164.58°.

Table 3
Selected bond distances (Å) and angles (°) for complex **3a**

Bond distances (Å)			
Fe(1)–O(61)	1.918(3)	Fe(2)–O(62)	1.914(3)
Fe(1)–O(62)	1.950(3)	Fe(2)–O(61)	1.950(3)
Fe(1)–O(21)	2.015(3)	Fe(2)–O(31)	2.009(3)
Fe(1)–O(1)	2.078(3)	Fe(2)–O(41)	2.053(3)
Fe(1)–O(11)	2.052(3)	Fe(2)–O(51)	2.069(3)
Fe(1)–N(1)	2.164(4)	Fe(2)–N(2)	2.164(4)
Fe(3)–O(61)	1.863(3)	Fe(4)–O(62)	1.869(3)
Fe(3)–O(32)	2.043(3)	Fe(4)–O(22)	2.049(3)
Fe(3)–O(12)	2.064(3)	Fe(4)–O(42)	2.049(3)
Fe(3)–O(2)	2.082(3)	Fe(4)–O(52)	2.083(3)
Fe(3)–N(3)	2.211(4)	Fe(4)–N(4)	2.210(4)
Fe(3)–Cl(1)	2.324(1)	Fe(4)–Cl(2)	2.327(1)
Angles (°)			
Fe(3)–O(61)–Fe(1)	124.42(15)	Fe(2)–O(62)–Fe(1)	97.36(12)
Fe(3)–O(61)–Fe(2)	131.22(15)	Fe(4)–O(62)–Fe(2)	124.08(15)
Fe(1)–O(61)–Fe(2)	97.23(12)	Fe(4)–O(62)–Fe(1)	131.25(15)
O(61)–Fe(1)–O(62)	82.22(12)	O(61)–Fe(1)–O(21)	172.69(12)
O(62)–Fe(1)–O(11)	177.19(12)	O(1)–Fe(1)–N(1)	168.34(13)
O(62)–Fe(2)–O(61)	82.30(12)	O(62)–Fe(2)–O(31)	172.77(12)
O(51)–Fe(2)–N(2)	167.94(13)	O(61)–Fe(3)–N(3)	173.14(14)
O(61)–Fe(2)–O(41)	176.33(13)	O(62)–Fe(4)–N(4)	171.20(16)
O(32)–Fe(3)–O(12)	164.40(12)	O(52)–Fe(4)–Cl(2)	174.17(10)
O(2)–Fe(3)–Cl(1)	173.70(9)	O(22)–Fe(4)–O(42)	165.47(13)
Separations			
Fe(1)···Fe(2)	2.902(1)	Fe(1)···Fe(4)	3.478
Fe(2)···Fe(4)	3.341	Fe(1)···Fe(3)	3.345
Fe(2)···Fe(3)	3.473	Fe(3)···Fe(4)	6.116

Thus, the core can be considered as two edge-sharing Fe_3 triangular units with the oxygen atoms out of their Fe_3 planes. Peripheral ligation is provided by six RCO_2^- groups and two chloride ions. The body/wing-tip Fe_2 pairs are bridged by six μ_2-carboxylate groups in *syn–syn* modes, while the two chloro ligands, are coordinated with each of the two wing metal ions Fe(3) and Fe(4). The metal ions are octahedrally coordinated with their chromophores being $FeO_6$and FeO_5Cl. The Fe···Fe separations fall into two types. The body/body separation, Fe(1)···Fe(2), is short (2.902(1) Å) as these metal ions are bridged by two oxo atoms. The wing-tip/body Fe···Fe separations can be distinguished into two types: those bridged by one (Fe(l)···Fe(4), 3.478 Å and Fe(2)···Fe(3), 3.473 Å) and those bridged by two carboxylato groups (Fe(1)···Fe(3), 3.345 Å and Fe(2)···Fe(4), 3.341 Å). Finally, the wing-tip/wing-tip separation (Fe(3)···Fe(4), 6.116 Å) is the longest as expected. The ''body''-Fe to μ_3-*O* distances are the same 1.950(3) Å, whereas the ''wing-tip''-Fe to μ_3-*O* distances are slightly shorter 1.863(3) and 1.869(3) Å. This symmetry is also reflected in the bond angles at the triply bonding oxo atoms: the Fe(1)–O(61)–Fe(2) and Fe(1)–O(62)–Fe(2) angles (97.23(12)° and 97.36(12)°, respectively) are much smaller than the other Fe(1)–O(61)–

Fe(3), Fe(2)–O(61)–Fe(3) angles (124.42(15) and 131.22(15)°) or Fe(4)–O(62)–Fe(2) and Fe(4)–O(62)–Fe(1) angles (124.08(15) and 131.25(15)°, respectively). The two chloro ligands are bound to Fe(3) and Fe(4) at 2.324(1) and 2.327(1) Å distances, respectively.

3.4. Artificial nucleolytic enzyme activity assay

Some compounds catalyze the hydrolysis of the phosphodiester backbone of DNA mimicking the naturally occurring endonucleases.The DNA degradation produces acid-soluble products giving an increase in the absorbance at 260 nm, while a diminution suggests an eventual formation of DNA–Fe(III) complex, resulting from the interaction of the iron clusters with DNA and precipitation with perchloric acid, allowing to determine the function of molecules capable to mimic the real endonuclease activity against DNA [77].The Fe(III) complexes were tested for the hydrolysis ability towards the native dsDNA. The degree of CT-DNA degradation was assessed by the release of acid-soluble oligonucleotides after incubation with these iron complexes.

When increasing amounts of dsDNA were assayed for acid-soluble products, an increase in the absorbance at 260 nm was measured (Fig. 3, curve ▼). A fixed amount of $[Fe_2O(mcpa)_2(bipy)_2Cl_2]$ (**1a**) (0.1 mM in dmso), under the same conditions, an absorbance of approximately $A = 0.8$ at 260 nm, exhibited. Upon incubation of increasing amounts of dsDNA with the pre-referred fixed amount of **1a**, a significant decrease of the initial absorbance at 260 nm of the acid-soluble products was obtained, attributed to the diminution of the oligonucleotides present in the supernatant and the free $[Fe_2O(mcpa)_2(bipy)_2Cl_2]$ cluster (Fig. 3, curve ▲). Thus, we can obtain the amount of free **1a** remaining in the supernatant by subtracting the values of curve ▼ from the corresponding values of curve ▲ ($A_{DNA + \{Fe\}} - A_{DNA}$). The obtained values were decreased when the amount of the DNA added in proportion increased (Fig. 3, curve ♦). Upon addition of 160 μg of DNA more than 60% of **1a** was removed from the supernatant that corresponds to the percentage $[Fe_2O(mcpa)_2(bipy)_2Cl_2]$ able to bind to the DNA and precipitate in the perchloric acid pellet. Nevertheless, **1a** showed no detectable nuclease activity towards DNA with this method, assigned to the low concentration of the complex.A higher concentration leads to a significant contribution of compound in absorbancy at 260 nm, inhibiting in a way the determination of acid-soluble deoxyribonucleotides.The hydrolysis of the phosphodiester bond of dinucleotides DNA substrates was cited using a concentration of metals as high as 10 mM [78]. It was really confirmed by the agarose gel electrophoresis study (see below) showing that the degradative effect of **1a**, which mimics endonucleolytic activity, was observed at a concentration that is 10-fold higher (at concentration of 1 mM, Fig. 5, lane 3). For example, the concentrations being used that show any effects at all are in the mM range, far to high to be biologically significant. If you add mM quantities of almost any metal complex effects on DNA would be observed.

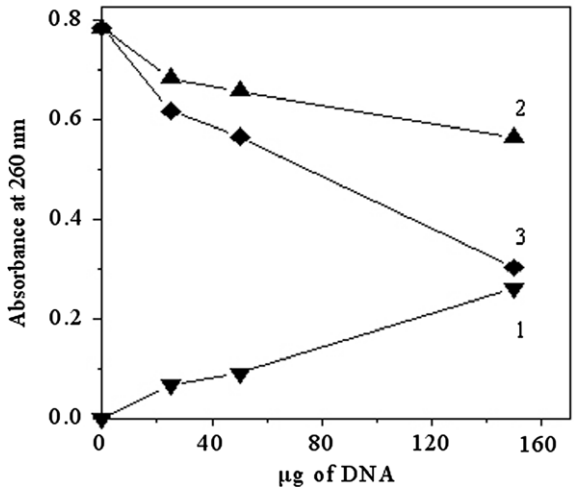

Fig. 3. Determination of acid-soluble deoxyribonucleotides by measuring the absorbance at 260 nm, after progressive addition of increased amounts of dsDNA in 0.1 mM of $[Fe_2O(mcpa)_2(bipy)_2Cl_2]$ (**1a**) in dmso and incubation for 30 min at 37 °C; (Curve ▼)The mixtures containing 5 mM Tris–HCl pH 7.5, 50 mM NaCl, 10% dmso and progressively increased amounts of calf thymus gland dsDNA added in proportion and incubated for 30 min at 37 °C. (Curve ▲) Corresponding mixtures of previously referred, supplemented with **1a** (0.1 mM in dmso); (Curve ◆) Acid-soluble products remained in the supernatant corresponding to the amount of the non-bound **1a**.

3.4.1. DNA binding studies by spectroscopic titration

In order to provide more evidence for the possibility of binding of $[Fe_2O(mcpa)_2(bipy)_2Cl_2]$ (**1a**) to double stranded DNA, the spectroscopic titration of a solution of **1a** with calf thymus DNA (CT-DNA), a classical method frequently used to evaluate the binding of intercalative drugs to the DNA helix [41,44,45] was performed.

Fig. 4 illustrates the spectral changes of **1a** in dmso solution upon addition of increasing amounts of CT-DNA. The initial spectrum (upper line) refers to the free $[Fe_2O(mcpa)_2(bipy)_2Cl_2]$ complex in the absence of CT-DNA. The following spectra were recorded after addition of CT-DNA in a proportion ranging from 5 to 265 μg CT-DNA to the assay mixture containing 3 mM of free $[Fe_2O(mcpa)_2(bipy)_2Cl_2]$.The addition of CT-DNA results in an hypochromism shift of the band centered at 485 nm, assigned to $p\pi \rightarrow Fe(III)d\pi^*$ charge transfer (CT) transition. Furthermore, the hypochromism is accompanied by a moderate hypsochromic shift of the maximum. Similar spectral changes were obtained at 480 nm, when CT-DNA was added in a proportion ranging from 2.5 to 82.5 μg CT-DNA to the assay mixture containing 1.5 mM of free $[Fe_2O(2,4,5\text{-}T)_2(phen)_2Cl_2]$ (data not shown).

In addition to gain more insights into the possibility of binding of **1a** to CT-DNA, spectrophotometric titration at the maximum absorbance of CT-DNA region (260–

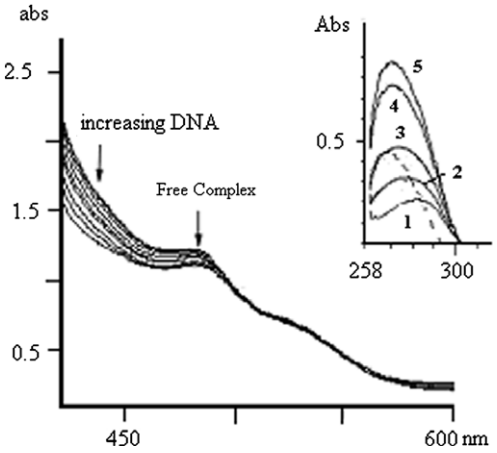

Fig. 4. Variation in metal-to-ligand charge transfer spectra of $[Fe_2O(mcpa)_2(bipy)_2Cl_2]$ (**1a**) in dmso upon increasing addition of CT-DNA in 5 mM Tris–HCl buffer (pH 7.5) and 50 mM NaCl and incubation for 30 min at 37 °C. The concentration of **1a** used was 3 mM and the amounts of DNA added were 5, 15, 25, 45, 65, 115, 165 and 265 μg of dsDNA respectively. (Inset) The concentration of $[Fe_2O(mcpa)_2(bipy)_2Cl_2]$ used was 1 mM and the amounts of DNA added were 5, 10, 20 and 30 μg of dsDNA respectively.

300 nm) was also performed.The inset of Fig. 4 shows the initial spectrum of the free $[Fe_2O(mcpa)_2(bipy)_2Cl_2]$ in dmso solution, i.e. in the absence of CT-DNA, exhibiting a maximum at 282 nm (curve 1). A solution of 20 μg/mL CT-DNA in dmso shows a maximum at 264 nm (doted line).The addition of increasing amounts of CT-DNA to the free $[Fe_2O(mcpa)_2(bipy)_2Cl_2]$ solution, ranging from 5 to 30 μg, resulted in a hypsochromic shift of the maximum of the free complex from 282 to 267 nm, depending on the amount of CT-DNA added. The results show that the amount of the free complex used is sufficient to saturate all available sites for binding in 5 (or −10 μg) of CT-DNA added (curves 2 and 3). Higher amounts of DNA completely masked the band of the maximum absorbance of the free complex and the hypsochromic shift was not observed. The fact that spectral changes at λ_{max} caused by the addition of CT-DNA to a solution containing $[Fe_2O(mcpa)_2(bipy)_2Cl_2]$ confirms the hypothesis for its interaction with DNA.

3.5. Interaction of iron complexes with dsDNA

It is known that iron complexes are able to promote hydrolytic cleavage of phosphodiester–DNA bonds especially under physiological pH conditions (6.1 and 8.0) [41,56]. Therefore, the effect of the Fe compounds on the integrity of the native calf thymus DNA (CT-DNA) was tested and assessed by gel electrophoresis stained with ethidium bromide. The experiments to achieve the cleavage of DNA were carried out at pH 7.5 using 50 mM Tris–HCl buffer. When CT-DNA was incubated with increasing concentrations of each of the compounds for 30 min at 37 °C, the CT-DNA was obviously degraded, in the presence of 1 mM of each of the dimeric compounds with bipy, almost in the same extent **1a** > **1c** > **1b** ($[Fe_2O(mcpa)_2(bipy)_2Cl_2]$ > $[Fe_2O(3,4\text{-}D)_2(bipy)_2Cl_2]$ > $[Fe_2O(2,4,5\text{-}T)_2(bipy)_2Cl_2]$). This conclusion was deduced by the diminution of the total initial amount of dsDNA used (Fig. 5, lane 3).

Similarly, when CT-DNA was treated with 1 mM of $\{[Fe_4O_2(mcpa)_6Cl_2(py)_4]\cdot 2MeCN\}$ (**3a**), $\{[Fe_4O_2(2,4,5\text{-}T)_6Cl_2(py)_4]\cdot 2MeCN\}$ (**3b**), and $\{[Fe_4O_2(3,4\text{-}D)_6Cl_2(py)_4]\cdot 2MeCN\}$ (**3c**), a partial migration of the main CT-DNA band to a higher molecular weight shown as a band on the top of the gel differing in intensity was observed, which barely came across the gel (Fig. 6, lane 3). Therefore, among the tetranuclear compounds the effectiveness seems to be in the order: **3c** > **3a** > **3b**. The different degrees of binding between the dimeric and tetrameric clusters may be the assigned to different modes of interaction swith DNA. It seems that dimeric clusters assault DNA with a degradative manner under these conditions deduced from the complete disappearence of the initial DNA (Fig. 5, lane 3), while tetrameric clusters with an intercalative (or other kind of binding) manner such as interstrand cross-links or covalent binding to nucleophilic centers of DNA concluded from the migration of the band located on the top of the gel (Fig. 6, arrow).

A comparative experiment performed in two different concentrations (Fig. 1S) showed that the degradative effect is concentration dependent since lower concentrations seem to be less or not at all effective on DNA. In addition, this effect is dependent on incubation time with the iron

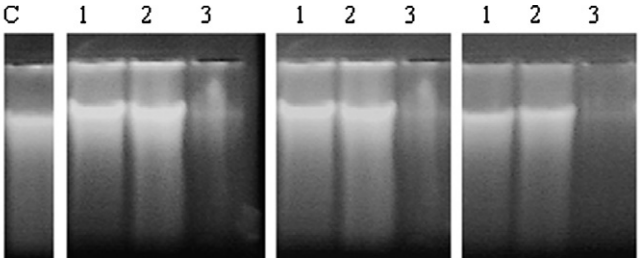

Fig. 5. Agarose (1%) gel electrophoresis of double stranded DNA. Each sample containing 3 μg of dsDNA treated with the indicated concentrations of compounds **1a**, **1c** and **1b** at 37 °C for 30 min; Lane 1: control, dsDNA without treatment; Lanes 1–3: dsDNA treated with 0.25, 0.5 and 1.0 mM of compounds **1a**, **1c** and **1b**, respectively.

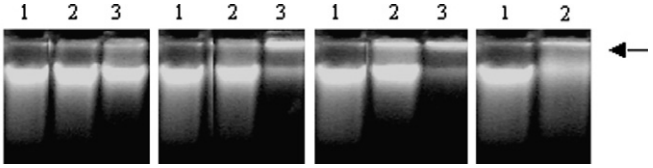

Fig. 6. Agarose (1%) gel electrophoresis of double stranded DNA. Each sample containing 3 μg of ds DNA was treated with the indicated concentrations of the compounds **3a**, **3c**, **3b** and **1f** at 37 °C for 30 min. Lane 1: control, dsDNA without treatment; Lanes 2–3: dsDNA treated with 0.5 and 1.0 mM of compound **3a**, **3c**, **3b** and 1.0 mM of compound **1d** (lane 2) respectively.

complexes. A longer incubation time resulted in a more extensive degradative effect exhibiting its maximum after 30 min of incubation (data not shown). The cleavage reaction does not require additional external agents. Even in the presence of dmso, which is a known radical scavenger the cleavage reaction occurred, suggesting that this cleavage is mediated by iron compounds in the absence of external coreactants and does not, in fact, occur via diffusible hydroxyl radicals (a classical oxidative mechanism). In conclusion, the results presented here lead us to conclude that the cleavage of DNA by the compounds is oxygen-independent and that this reaction most probably occurs through a hydrolytic mechanism. In a previous report [41] it was proposed that the hydrolytic cleavage of DNA is most probably facilitated by the hydrophobic interaction of the pyridine and phenolate iron-coordinated ligands with the nitrogen base pairs easily accessed from B-DNA major groove.

3.6. Interaction of iron-complexes with pDNA

We have also examined the ability of the compounds to unwind or condense a supercoiling substrate such as plasmid DNA. Fig. 7 shows agarose gel electrophoresis patterns for the interaction of pDNA with Fe(III) compounds. When pDNA was incubated with each of them, a migration of both bands of the plasmid (supercoiled and relaxed) was observed (Fig. 7, lanes 3–7) to higher molecular weight bands with the concomitant formation of new products (Fig. 7, lanes 3–7 and 9). This fact may be the result of an eventual cross-linking of pDNA with many molecules of the corresponding compounds. These aggregates reflect a reduced electrophoretic mobility compared to both forms of supercoiled and relaxed pDNA. This shift is clearly obvious in Fig. 7, lane 7 (compound **2a**) and secondly in lanes 4–6 (compounds **3b**, **3a**, **3c**). It should be noted that the reaction was performed in the presence of dmso (which is the solute of all the compounds and it is known as a potential radical scavenger).

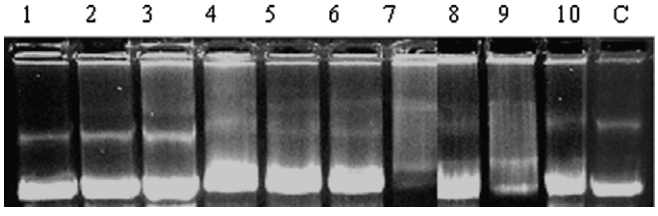

Fig. 7. Agarose (1%) gel electrophoresis of plasmid DNA. Each sample containing 3 μg of pDNA was treated with 1 mM of the iron compounds at 37 °C for 30 min. Lanes 1–3: pDNA treated with 1.0 mM of compounds **1c**, **1b, 1a**; Lanes 4–6: pDNA treated with 1.0 mM of compounds **3b**, **3a**, **3c**; Lane 7: pDNA treated with 1.0 mM of compound **2a**; Lanes 8–10: pDNA treated with 1.0 mM of compounds **1d**, **1e** and **3d**; Lane C: control, pDNA without treatment.

3.7. Antimicrobial activity

The minimum inhibitory concentrations of the complexes against *S. aureus*, *E. coli*, *B. subtilis* and *P. bulgaris* are listed in Table 4.

Free ligands (3,4-D, 2,3-D, 2,4,5-T, mcpa, bipy, py, phen) exhibited a >800 μg/mL MIC against the same microorganisms. The results do not indicate any specificity against $Gram^+$ or $Gram^-$ bacteria.

For metal complexes showing antimicrobial activity, five principal factors have been considered [70]. (i) The chelate effect. Ligands like bipy, phen, bipyam, bound to metal ions in a bidentate fashion show a higher antimicrobial efficiency towards complexes with unidentate N-donor ligands e.g. py; (ii) The total charge of the complex. Generally the antimicrobial efficiency decreases in the order cationic > neutral > anionic complex. This behaviour may be related to the redox potential which decreases in the same order; (iii) The nature of the ion neutralizing the ionic complex; (iv) The nature of the N-donor ligands; and (v) The nuclearity of the metal center in the complex [69].

We have initiated studies on the antimicrobial activity of manganese and copper complexes. The simple manganese herbicide or carboxylato complexes have shown a relatively weak antimicrobial behaviour while manganese polynuclear compounds, known as metallacrowns [71], were more active. $Mn(II)(2,4,5\text{-}T)_2[15\text{-}MC_{Mn(III)N(shi)}\text{-}5](py)_6$ was the most potent among all metallacrown compounds tested (MIC = 50 μg/mL against all microorganisms) [71]. The comparison of the MIC values of the $[12\text{-}MC_{Mn(III)N(shi)}\text{-}4]$ and $[15\text{-}MC_{Mn(III)N(shi)}\text{-}5]$ metallacrowns suggests that an increase in the metallacrown ring size results in an increased antimicrobial activity [44]. It was shown that among the copper complexes with the formulas [Cu(N-donor ligand)$_2$L]Cl, [Cu(L)(N-donor ligand)$_2$]Cl and Cu_2(N-donor ligand)$_2$(L)$_4$, the most efficient class of com-

Table 4
Minimum inhibitory concentration, (M.I.C.) of selected Fe(III) compounds in μg/mL

Compound	*Escherichia coli* Gram (−)	*Proteus bulgaris* Gram (−)	*Staphylococcus aureus* Gram (+)	*Bacillus subtilis* Gram (+)
1a	100	50	50	100
1b	100	50	100	50
1c	100	50	50	25
1d	100	50	12.5	100
1e	100	50	50	12.5
1f	50	100	25	50
2a	200	200	200	200
2b	400	200	200	200
2c	200	200	400	200
3a	50	100	200	100
3b	50	200	100	100
3c	200	50	100	100
3d	400	400	200	200
3e	400	200	400	200
3f	200	200	400	200

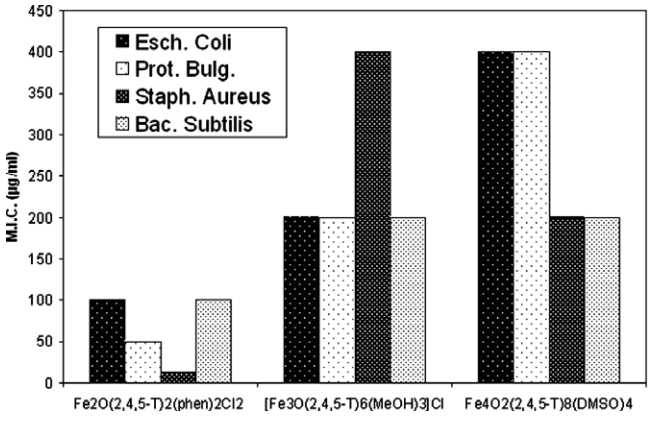

Fig. 8. Antimicrobial activity, expressed as MIC (μg/mL), of the dinuclear, trinuclear and tetranuclear complexes with the same ligand (*2,4,5T*) against *Staphylococcus aureus*, *Escherichia coli*, *Bacillus subtilis* and *Proteus bulgaris*.

pounds is that with an ionic form, which exhibit the best inhibition (MIC = 100 μg/mL) against *S. aureus*, *E. coli*, *B. subtilis* and *P. bulgaris* [57].

In the present study, we have considered the chelate effect and the nuclearity of a series of polynuclear ferric compounds showing antimicrobial activity as principal factors. A comparison of the MIC values of the ferric herbicide complexes suggests that the nuclearity does not affect the overall behaviour of the compounds (Table 4). Trinuclear and tetranuclear complexes having monodentate solvent-molecules as ligands show similar behaviour while the presence of N-chelate neutral ligand in dinuclear compounds results in a significant increase of the antimicrobial activity (Fig. 8). This conclusion is based on the fact that a blank test of propylenoglycol or dmso showed no antimicrobial action.

4. Conclusions

The structural characterization of bi- and tetranuclear Fe(III) complexes confirms the ability of alkanoato ligands to give a variety of multinuclear complexes. The formation of binuclear compounds is driven by the presence of chelating bipy or phen neutral ligands. The use of methanol leads to the formation of the trinuclear species while from dmso, py or dmf solvents the tetranuclear compounds have been isolated.The determination of acid-soluble deoxyribonucleotides showed that more than 60% of the $[Fe_2O(mcpa)_2(bipy)_2Cl_2]$ can be bound to DNA while spectroscopic titration studies with calf thymus DNA suggests strength of the binding of the complex to the DNA helix. The results of agarose gel electrophoresis of dsDNA suggest that the cleavage of DNA by the Fe(III) compounds is oxygen-independent and most probably occurs through a hydrolytic mechanism. Reduced electrophoretic mobility of supercoiled and relaxed pDNA may be assigned to an eventual cross-linking of pDNA with many molecules of the Fe(III) clusters.The comparison of the MIC values showed that trinuclear and tetranuclear complexes having monodentate solvent-molecules as ligands show similar behaviour, while the presence of N-chelate neutral ligands in dinuclear compounds results in a significant increase of the antimicrobial activity.

Acknowledgement

The project is co-funded by the European Social Fund & National Resources-EPEAEK II-Archimidis I 2003/21.

Appendix A. Supplementary data

Analytical and spectroscopic data of all the compounds and CIF files for **1a** (CCDC 297100) and **3a** (CCDC 297101) containing the supplementary crystallographic data for this paper. The CIF files data can be obtained free of charge at www.ccdc.cam.ac.uk/conts/retrieving.html [or from the Cambridge Crystallographic Data Centre, 12 Union Road, Cambridge CB2 1EZ, UK; fax: +44 1223 336033; e-mail: deposit@ccdc.cam.ac.uk]. Ordering and access information is given on any current masthead page. Supplementary data associated with this article can be found, in the online version, at doi:10.1016/j.ica.2006.07.102.

References

[1] D.M. Kurtz Jr., J. Biol. Inorg. Chem. 2 (1997) 159.
[2] M.A.J. Homes, R.E. Stenkamp, J. Mol. Biol. 220 (1991) 723.
[3] L. Que Jr., J. Chem. Soc., Dalton Trans. (1997) 3933.
[4] D.T. Logan, X.-D. Su, A. Aberg, K. Regnsträn, J. Hajdu, H. Eklund, P. Nordlund, Structure 4 (1996) 1053.
[5] A.C. Rosenzweig, P. Nordlund, P.M. Takahara, C.A. Frederick, Chem. Biol. 2 (1995) 409.
[6] J.B. Vincent, G.-L. Olivier-Lilley, B.A. Averill, Chem. Rev. 90 (1990) 1447.
[7] L. Que Jr., Chem. Rev. 96 (1996) 2607.
[8] Y. Lindqvist, E. Jonhansson, H. Kaija, P. Vihko, G. Schneider, J. Mol. Biol. 291 (1999) 135.
[9] L.W. Guddat, A.S. McAlpine, H. Hume, S. Hamilton, J. de Jersey, J.L. Martin, Structure 7 (1999) 757.
[10] G.A. Clegg, J.E. Fitton, P.M. Harrison, A. Treffry, Prog. Biophys. Mol. Biol. 36 (1980) 53.
[11] E.C. Theil, Annu. Rev. Biochem. 56 (1987) 289.
[12] P.M. Harrison, P. Arosio, Biochim. Biophys. Acta 1275 (1996) 161.
[13] A.K. Boudalis, C.P. Raptopoulou, A. Terzis, S.P. Perlepes, Polyhedron 23 (2004) 1271.
[14] J.B. Vincent, J.C. Huffman, G. Christou, Q. Li, M.A. Nanny, D.N. Hendrickson, R.H. Fong, R.H. Fish, J. Am. Chem. Soc. 110 (1988) 6898.
[15] K.L. Taft, A. Maschelein, S. Liu, S.J. Lippard, D. Garfinkel-Shweky, A. Bino, Inorg. Chim. Acta 198 (1992) 627.
[16] S. Ménage, J.-M. Vincent, C. Lambeaux, G. Chottard, A. Grand, M. Fontecave, Inorg. Chem. 32 (1993) 4766.
[17] J. Li, J. Zou, M. Wu, Z. Xu, X. You, T.C.W. Mak, Polyhedron 14 (1995) 3519.
[18] A. Neves, M.A. de Brito, I. Vencato, V. Drago, K. Griesar, W. Haase, Inorg. Chem. 35 (1996) 2360.
[19] E. Lambert, B. Chabut, S. Chardon-Noblat, A. Deronzier, G. Chottard, A. Bousseksou, J.P. Tuchagues, J. Laugier, M. Bardet, J.M. Latour, J. Am. Chem. Soc. 119 (1997) 9424.

[20] E. Bernard, S. Chardon-Noblat, A. Deronzier, J.M. Latour, Inorg. Chem. 38 (1999) 190.
[21] A. Neves, L.M. Rossi, I. Vencato, W. Haase, R. Werner, J. Chem. Soc., Dalton Trans. (2000) 707.
[22] M. Laznaster, A. Neves, A.J. Bortoluzzi, B. Szpoganicz, E. Schwingel, Inorg. Chem. 41 (2002) 5641.
[23] P. Karsten, A. Neves, A.J. Bortoluzzi, V. Drago, M. Laznaster, Inorg. Chem. 41 (2002) 4624.
[24] A.K. Powell, S.L. Heath, D. Gatteschi, L. Pardi, R. Sessoli, G. Spina, F.D. Giallo, F. Pieralli, J. Am. Chem. Soc. 117 (1995) 2491.
[25] S.M. Oh, D.N. Hendrickson, K.L. Hasset, R.E. Davis, J. Am. Chem. Soc. 107 (1985) 8009.
[26] D.P. Goldberg, J. Tesler, C.M. Bastos, S.J. Lippard, Inorg. Chem. 34 (1995) 3011.
[27] A.M. Bond, R.J.H. Clark, D.G. Humphrey, P. Panayiotopoulos, B.W. Skelton, A.H. White, J. Chem. Soc., Dalton Trans. (1998) 1845.
[28] J.K. McCusker, J.B. Vincent, E.A. Schmitt, M.L. Mino, K. Shin, D.K. Coggin, P.M. Hagen, J.C. Huffman, G. Christou, D.N. Hendrickson, J. Am. Chem. Soc. 113 (1991) 3012.
[29] R.A. Stukan, V.I. Ponomarev, V.P. Nifontov, K.I. Turte, L.O. Atovmyan, J. Struct. Chem. 26 (1985) 197.
[30] D.L. Jameson, C.-L. Xie, D.N. Hendrickson, J.A. Potenza, H.J. Schugar, J. Am. Chem. Soc. 109 (1987) 740.
[31] B. Yan, Z.-D. Chen, Inorg. Chem. Commun. 4 (2001) 138.
[32] M.W. Wemple, D.K. Coggin, J.B. Vincent, J.K. McCusker, W.E. Streib, J.C. Huffman, D.N. Hendrickson, G. Christou, J. Chem. Soc., Dalton Trans. (1998) 719.
[33] W.H. Armstrong, M.E. Roth, S. Lippard, J. Am. Chem. Soc. 109 (1987) 6318.
[34] P. Chaudhuri, M. Winter, P. Fleischhauer, W. Haase, U. Florke, H.-J. Haupt, Inorg. Chim. Acta 212 (1993) 241.
[35] L. Wu, P. Pressprich, P. Coppens, M.J. DeMarco, Acta Crystallogr., Sect. C 49 (1993) 1255.
[36] R.A. Reynolds, W.R. Dunham, D.C. Coucouvanis, Inorg. Chem. 37 (1998) 1232.
[37] V.I. Ponomarev, L.O. Atovmyan, S.A. Bobkova, K.I. Turte, Dokl. Akad. Nauk. SSSR 274 (1984) 368.
[38] S.M. Gorun, S.J. Lippard, Inorg. Chem. 27 (1988) 149.
[39] R. Celenligil-Cetin, R.J. Staples, P. Stavropoulos, Inorg. Chem. 39 (2000) 5838.
[40] A.K. Boudalis, N. Lalioti, G.A. Spyroulias, C.P. Raptopoulou, A. Terzis, A. Bousseksou, V. Tangoulis, J.-P. Tuchagues, S.P. Perlepes, Inorg. Chem. 41 (2002) 6474.
[41] A. Horn Jr., I. Vencato, A.J. Bortoluzzi, R. Horner, R.A. Nome Silva, B. Spoganicz, V. Drago, H. Terenzi, M.C.B. de Oliviera, R. Werner, W. Haase, A. Neves, Inorg. Chim. Acta 358 (2005) 339.
[42] C. Liu, S. Yu, D. Li, Z. Liao, X. Sun, H. Xu, Inorg. Chem. 41 (2002) 913.
[43] M. Scarpellini, A. Neves, R. Horner, A.J. Bortoluzzi, B. Spoganicz, C. Zucco, R.A. Nome Silva, V. Drago, A.S. Mangrich, W.A. Ortiz, W.A.C. Passos, M.C.B. de Oliviera, H. Terenzi, Inorg. Chem. 42 (2003) 8353.
[44] S. Mahadevan, M. Palaniandavar, Inorg. Chem. 37 (1998) 693.
[45] H. Chao, W.-J. Mei, Q.-W. Huang, L.-N. Ji, J. Inorg. Biochem. 92 (2002) 165.
[46] A. Neves, H. Terenzi, R. Horner, A. Horn Jr., B. Szpoganicz, J. Sugai, Inorg. Chem. Commun. 4 (2001) 388.
[47] B. Norden, F. Tjerneld, FEBS Lett. 67 (1976) 368.
[48] T. Hard, B. Norden, Biopolymers 25 (1986) 1209.
[49] T. Hard, C. Hiort, B. Norden, J. Biomol. Struct. Dyn. 5 (1987) 89.
[50] J.G. Collins, R.M. Rixon, J.R. Aldrich-Wright, Inorg. Chem. 39 (2000) 4377.
[51] R.E. Holmin, J.K. Barton, Inorg. Chem. 34 (1995) 7.
[52] R.H. Terbrueggen, T.W. Johann, J.K. Barton, Inorg. Chem. 37 (1998) 6874.
[53] R.E. Holmin, J.A. Yao, J.K. Barton, Inorg. Chem. 38 (1999) 174.
[54] S. Arounaguiri, B.G. Maiya, Inorg. Chem. 35 (1996) 4267.
[55] V.W.-w. Yam, K.K.-w. Lo, K.-k. Cheung, R.Y.-c. Kong, J. Chem. Soc., Dalton Trans. (1997) 2067.
[56] Mudasir, K. Wijaya, N. Yoshioka, H. Inoue, J. Inorg. Biochem. 94 (2003) 263.
[57] C. Dendrinou-Samara, L. Alevizopoulou, L. Iordanidis, E. Samaras, D.P. Kessissoglou, J. Inorg. Biochem. 89 (2002) 89.
[58] C. Dendrinou-Samara, G. Psomas, K. Christophorou, V. Tangoulis, V.P. Raptopoulou, A. Terzis, D.P. Kessissoglou, J. Chem. Soc., Dalton Trans. (1996) 3737.
[59] G. Psomas, C. Dendrinou-Samara, P. Philippakopoulos, V. Tangoulis, C.P. Raptopoulou, H. Samaras, D.P. Kessissoglou, Inorg. Chim. Acta 272 (1998) 24.
[60] C. Dendrinou-Samara, G. Tsotsou, C.P. Raptopoulou, A. Kortsaris, D. Kyriakidis, D.P. Kessissoglou, J. Inorg. Biochem. 71 (1998) 171.
[61] G. Psomas, C.P. Raptopoulou, L. Iordanidis, C. Dendrinou-Samara, V. Tangoulis, D.P. Kessissoglou, Inorg. Chem. 39 (2000) 3042.
[62] I. Tsivikas, M. Alexiou, A.A. Pantazaki, C. Dendrinou-Samara, D.A. Kyriakidis, D.P. Kessissoglou, Bioinorg. Chem. Appl. 1 (2003) 85.
[63] M. Alexiou, I. Tsivikas, C. Dendrinou-Samara, A. Pantazaki, P. Trikalitis, N. Lalioti, D.A. Kyriakidis, D.P. Kessissoglou, J. Inorg. Biochem. 93 (2003) 256.
[64] M.A. Zoroddu, S. Zanetti, R. Pogni, R. Basosi, J. Inorg. Biochem. 63 (1996) 291.
[65] M. Ruiz, L. Perello, J. Servercarrio, R. Ortiz, S. Garciagranda, M.R. Diaz, E. Canton, J. Inorg. Biochem. 69 (1998) 231.
[66] F. Hueso-Urena, M.N. Moreno-Carretero, M.A. Romero-Molina, J.M. Salas-Peregrin, M.P. Sanchez-Sanchez, G. Alvarez de Cienfuegos-Lopez, R. Faure, J. Inorg. Biochem. 51 (1993) 613.
[67] A.M. Ramadan, J. Inorg. Biochem. 65 (1997) 183.
[68] M. Melnik, M. Auderova, M. Holko, Inorg. Chim. Acta 67 (1982) 117.
[69] G. Plesch, M. Blahova, J. Kratsmar-Smogrovic, C. Friebel, Inorg. Chim. Acta 136 (1987) 117.
[70] S.S. Block (Ed.), Disinfection, Sterilization and Preservation, fourth ed., Lea & Febinger, Philadelphia, 1991 (a) A.D. Russell, pp. 27–59; (b) H.W. Rossmore, pp. 290–321.
[71] C. Dendrinou-Samara, A.N. Papadopoulos, D. Malamatari, A. Tarushi, C. Raptopoulou, A. Terzis, E. Samaras, D.P. Kessissoglou, J. Inorg. Biochem. 99 (2005) 864.
[72] A. Chaudhary, N. Bansal, A. Gajraj, R.V. Singh, J. Inorg. Biochem. 96 (2003) 393.
[73] M. Palicova, P. Segl'a, D. Miklos, M. Kopcova, M. Melnik, B. Dubova, D. Hudecova, T. Glowiak, Polyhedron 19 (2000) 2689.
[74] M. Melnik, M. Koman, D. Hudecova, J. Moncol, B. Dubova, T. Glowiak, J. Mrozinski, C.E. Holloway, Inorg. Chim. Acta 308 (2000) 1.
[75] A. Valent, M. Melnik, D. Hudecova, B. Dubova, R. Kivekas, M.R. Sundberg, Inorg. Chim. Acta 340 (2002) 15.
[76] C. Dendrinou-Samara, S. Katsamakas, C.P. Raptopoulou, A. Terzis, V. Tangoulis, D.P. Kessissoglou, submitted for publication.
[77] (a) F. Mancin, P. Scrimin, P. Tecilla, U. Tonellato, Chem. Commun. (2005) 2540;
(b) C.P. Raptopoulou, S. Paschalidou, A.A. Pantazaki, A. Terzis, S.P. Perlepes, Th. Lialiaris, E.G. Bakalbasis, J. Mrozinski, D.A. Kyriakidis, J. Inorg. Biochem. 71 (1998) 15.
[78] A. Sreedhara, J.A. Cowan, J. Biol. Inorg. Chem. 6 (2001) 337.
[79] G.M. Sheldrick, SADABS, University of Göttingen, Germany.
[80] G.M. Sheldrick, SHELXS-86: Structure Solving Program, University of Göttingen, Germany, 1986.
[81] G.M. Sheldrick, SHELXL-97: Crystal Structure Refinement Program, University of Göttingen, Germany, 1997.